KAWASAKI STEEL TECHNICAL REPORT
No.3 (September 1981)

Continuous Casting of Beam Blanks

Masayuki Onishi, Tetsuo Ueda, Yutaka Shinjo, Hisakazu Mizota, Minoru Yao, Toshio Fujimura

Synopsis :
No.3 continuous casting machine at No.1 steel-making shop in Mizushima Works of Kawasaki Steel Corp., has a world's unprecedented dualrole feature of casting large-section blooms and beam blanks both. The machine has been successfully operating since October, 1973. In continuous coating of beam blanks, various kinds of defects are liable to occur due mainly to their complex forms, but nowadays improvement in cooling conditions, adoption of suitable mold powders and improved maintenance of the machine have made it possible of process almost all cast blanks into many different shapes without any conditioning. Casting speed has also been increased without any quality degradation by adopting a suitable cast supporting method for preventing flange deformation of cast blanks, after calculation of stress distribution of the solidified shell and studying a new method of supporting cast blanks. Operational results are as follows: (1) Casting time ratio: 90.6% (2) Frequency of breakouts: 0.02% (3) Yield of cast blanks: 99.6% (4) No surface conditioning ratio: 99% or higher

The body can be viewed from the next page.

Continuous Casting of Beam Blanks*

Masayuki ONISHI** Tetsuo UEDA** Yutaka SHINJO***
Hisakazu MIZOTA** Minoru YAO** Toshio FUJIMURA**

No. 3 continuous casting machine at No. 1 steel-making shop in Mizushima Works of Kawasaki Steel Corp., has a world's unprecedented dualrole feature of casting large-section blooms and beam blanks both. The machine has been succesfully operating since October, 1973.

In continuous casting of beam blanks, various kinds of defects are liable to occur due mainly to their complex forms, but nowadays improvement in cooling conditions, adoption of suitable mold powders and improved maintenance of the machine have made it possible to process almost all cast blanks into many different shapes without any conditioning.

Casting speed has also been increased without any quality degradation by adopting a suitable cast supporting method for preventing flange deformation of cast blanks, after calculation of stress distribution of the solidified shell and studying a new method of supporting cast blanks.

Operational results are as follows:

(1) Casting time ratio : 90.6%
(2) Frequency of breakouts : 0.02%
(3) Yield of cast blanks : 99.6%
(4) No surface conditioning ratio: 99% or higher

1 Introduction

The recent progress in continuous casting of steel has been remarkable as demonstrated by a noticeable rise in the continuous casting ratio. Various kinds of developments have been made aimed at achieving high efficiency of operation and high quality of products.

One of such developments is the "continuous casting of steel of a deformed cross section in a shape as close as possible to the final product". Continuous casting of beam blanks is one of its typical examples.

No. 3 continuous casting machine at Mizushima Works, which was designed after the beam blank CC machine of Algoma, has a dual-role capacity of casting large-section blooms and beam blanks both as the first of its kind in the world. Since its start-up in October 1973, the machine has been operating successfully with types of steel for continuous casting increased owing to improvement in the quality of steel. The productivity of continuous casting machine has been expanded due to increases in the number of heats in sequence and in casting speed[1-4].

As can be seen from its shape, the beam blank is considerably different from bloom or slab in internal stress and solidification mechanism during cooling, and its internal and surface properties are sensitively affected by operating conditions.

With improvements in the cooling conditions, selection of most suitable powders, and improved machine maintenance, all blanks are now sent to the subsequent process without conditioning and rolled into various shapes. Hot charging is also performed as long as a rolling schedule is availalbe for the cast.

This report describes the facilities and operation of beam blank continuous casting, especially defects in quality of products arising from high-speed casting and measures for correcting such defects.

2 Continuous Casting Machine for Beam Blanks

Table 1 shows general specifications of No. 3 continuous casting machine at Mizushima Works, and **Fig. 1** illustrates the size of a beam blank together with names of its various parts.

Charasteristic features of No. 3 continuous casting machine are as follows:

(1) Employment of the 2-point unbending system to prevent cracks caused by unbending of the solidify-

* Originally published in *Kawasaki Seitetsu Giho*, 12 (1980) 3, pp. 10–23 and rearranged with some modifications
** Mizushima Works
*** Research Laboratories

Table 1 General specifications of the continuous casting machine for beam blanks and blooms

Steel furnace	3 LD converter units
Furnace capacity	180 t (max.200 t)
Type of steel to be cast	C≦0.80%, Mn≦1.50%
Type	All upper-ground curved type
Number of strands	4
Strand center distance	2.2 m/2.4 m/2.2 m
Beam blank sizes	400 mm×460 mm×120 mm 287 mm×560 mm×120 mm*
Bloom dimensions	240 mm×400 mm,300 mm×400 mm, 400 mm×560 mm
Bending radius	12 500 mm, 22 000 mm
Pinch roll	Multi-type, 2-point unbending type
Length from meniscus to torch cutter	41 636 mm
Cutting length	4 000 mm-12 000 mm
Total height of facilities	Casting floor: FL+13 500 mm Pass line: FL+ 3 150 mm
Casting time	Approximately one hour/heat
Cutter	Messer type gas cutter, 2/strand

*Future operations

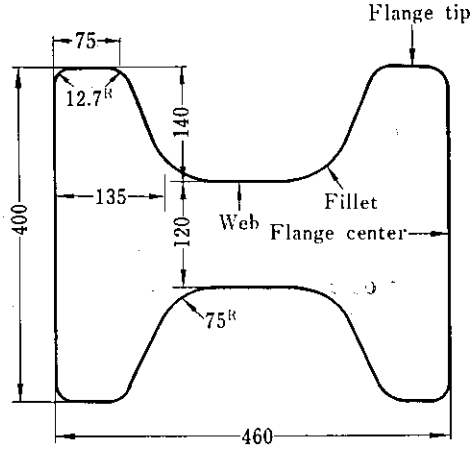

Fig. 1 Names and size of continuously cast beam blank

ing strand of high grade steel with a large cross section

(2) Dual-role capacity for casting both blooms and beam blanks

Hereunder main specifications for the beam blank CC machine are described.

2.1 Tundish

As shown in **Fig. 2,** the tundish is of the 4 strands type and has a trunnion distance of as long as 9 500 mm. In order to prevent deformation of a tundish, the tundish in the casting position is supported by the 3-point supporting system in which a hydraulic cylinder supports the center of the tundish in addition to trunnions at both sides.

The tundish is provided with 2 pouring ports per mold, and each nozzle has no flow control devices such as stopper and sliding gate. A quantity of molten steel is controlled by selecting nozzle bores.

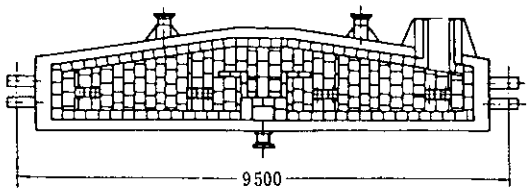

Fig. 2 Tundish

2.2 Mold

Fig. 3 shows the schematic drawing of the mold for a beam blank. The mold is divided into two pieces that are joined at the flange centers.

The mold is provided with a γ-ray level meter employing Co^{60} to control the level of meniscus automatically.

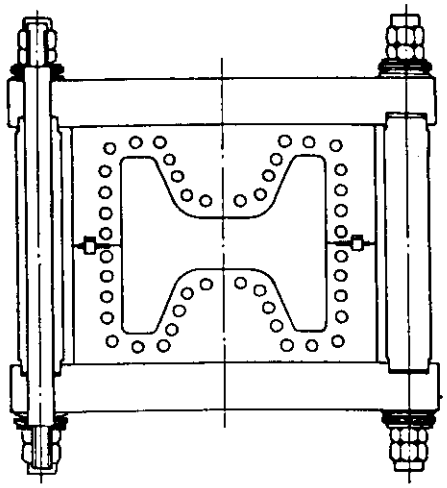

Fig. 3 Schematic drawing of the mold for beam blank

2.3 Roller Apron

The schematic drawing of the roller apron is shown in **Fig. 4.**

In order to prevent bulging, the roller apron is of a

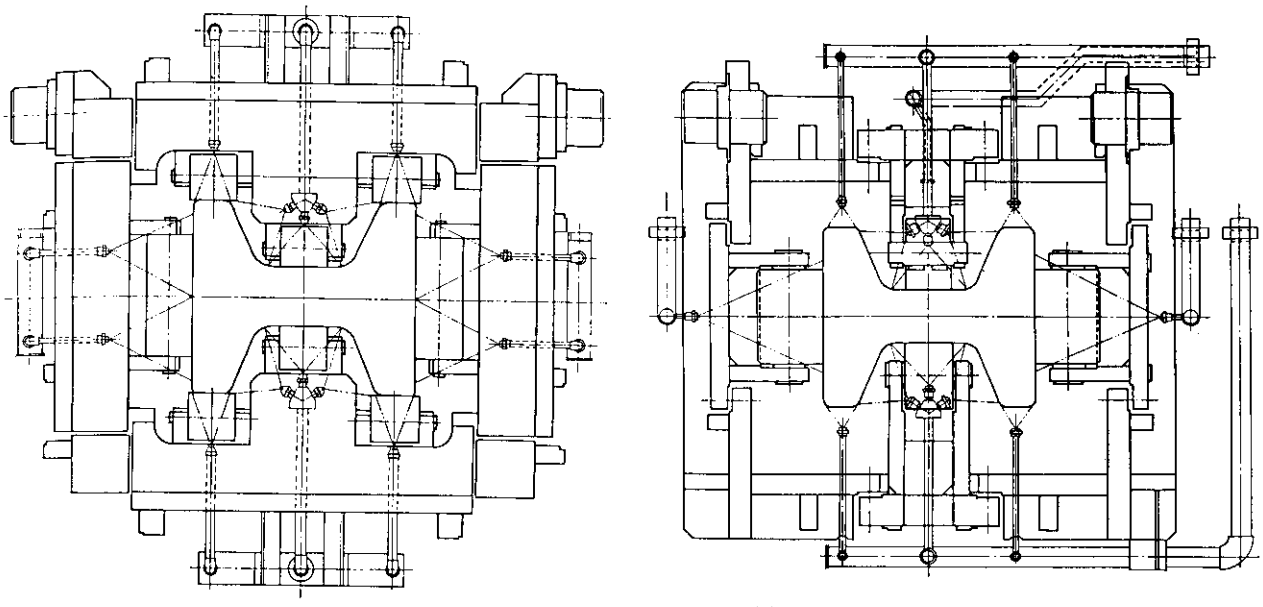

(a) Cross section of No.1 roller apron

(b) Cross section of No.2 and No.3 roller aprons

Fig. 4 Cross section of roller apron

complex construction with rolls for supporting flanges, flange tips and webs and with spray nozzles for cooling.

The roller apron for a distance of 8 m below the meniscus is divided into 3 segments which are exclusively used for beam blanks or blooms, while the roller aprons below 8 m are commonly used for both blooms and beam blanks. Thickness adjustment can be made by remote control.

In order to change the mold size quickly, a mold, oscillation guide and Nos. 1 and 2 segments are incorporated into a single frame, and then this frame and No. 3 segment are each simultaneously replaced with new units by using the main and auxiliary winding units of the overhead crane.

2.4 Dewatering Device

Since part of cooling water sprayed on the strand flows down the web inside of the bow of the beam blanks, it is necessary to purge the water by this dewatering unit.

3 Steel Grades and Their Casting Conditions

Table 2 shows the type of steel to be cast by the beam blank caster and casting conditions. **Fig. 5**

Table 2 Types of materials cast by B. B. caster and casting conditions

Type of material	Steel grade	Shield		Casting speed (m/min)	Spray cooling rate (*l*/kg)
		Ladle-tundish	Tundish-mold		
General structure	40 kg/mm² 50 kg/mm²	Open	Open + Semi-immersed nozzle	1.0-1.2	1.25
				0.85	0.92
Atomospheric corrosion resistant steel for welded structure	40 kg/mm² 50 kg/mm²	Open or Shrouding nozzle	Open + Semi-immersed nozzle or immersed nozzle	1.0-1.2	1.25
				0.85	0.92
Marine environments	Steels as designated in ASTM A690			0.75	1.27
Sheet pile of flat type	SY30,SY40 as designated in JIS	Open	Open + Semi-immersed nozzle	0.85	0.92

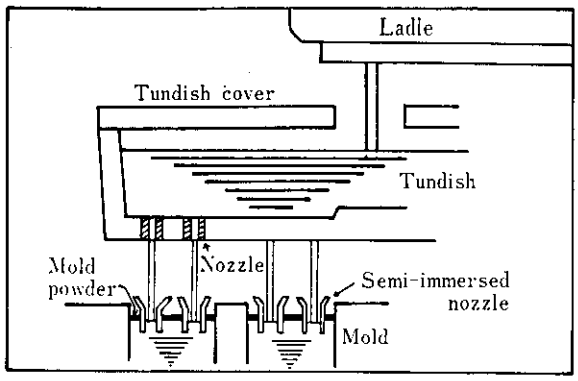

Fig. 5 Schematic representation of casting

shows the schematic representation of casting 40 kg/mm² grade steel .Non-shield casting is used between the ladle and the tundish and between the tundish and the mold.

With the aim of improving surface quality, mold powder is used, and in order to prevent powder inclusion, shallow-immersed nozzles (semi-immersed nozzles) are used only for the meniscus.

Although defects caused by nonmetallic inclusions in continuous casting of beam blanks are rarely observed, the consecutive casting stream of high grade steel such as fine grained steel is shielded by tundish submerged nozzle and semi-immersed nozzle made from alumina-graphite with gas bubbling at the upper part[5].

Results of investigation on the effects of the semi-immersed nozzle shape upon the occurrence of large-sized inclusions are shown in **Fig. 6**.

In this figure, the large-sized inclusion index is shown with the distance from the strand surface and the inclusion index. Rough sketches of semi-immersed nozzles are also shown in the figure.

It is observed that a 2-hole or 3-hole nozzle is more effective in reducing inclusions than a single-hole nozzle.

The 2-hole nozzle is used for supplying molten steel to the flange tips, while the 3-hole nozzle is used for supplying molten steel to the flange tips and webs, but no difference between them is observed regarding their effects on reducing large-sized inclusions.

Table 3 shows the typical defects of beam blanks and their preventive methods[3].

One of the typical surface defects of a beam blank is longitudinal cracks on the web surface.

According to the results of microscopic examination of the longitudinal cracks of the web, internal oxidization and de-carbonization are observed. These defects are assumed to be cracking defects developed in the mold, same as the longitudinal cracks of the slab and bloom. As already reported in the Kawasaki Steel Technical Report[3], the longitudinal cracks on the web surface are greatly affected by such factors as the composition of molten steel, properties of mold powder, deviation from the machine radius caused by mold oscillation, quantity of mold cooling water, shape of the mold cooling slit, and quantity of secondary cooling water. Controlling of these factors is therefore considered important. **Fig. 7** shows an example of relationship between the mold deviation from the machine radius caused by mold oscillation and the longitudinal surface cracking. Further, the temperature of mold cooling water influences the longitudinal cracks on the web surface, and the cracks occur more frequently as the temperature of the mold cooling water drops.

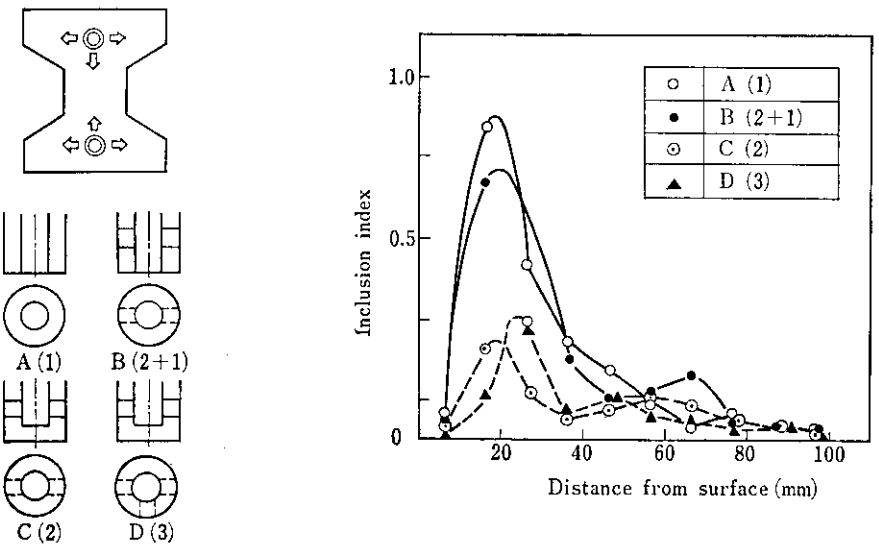

Fig. 6 Effect of the shape of immersed nozzle on the distribution of large inclusions in beam blank casting

In each case, since the solidified shell is more uniformly formed, the generating ratio of the longitudinal cracks on the web surface seems to be reduced.

Table 3 Typical defects of beam blanks and their prevention

Longitudinal facial cracks in web 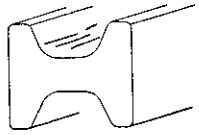	Decreasing sulfur content in steel Adoption of appropriate mold powder Minimizing the deviation of mold oscillation Appropriate cooling in a mold Mild cooling in upper secondary Appropriate spray distribution in spray cooling zone cross section
Longitudinal facial cracks in flange 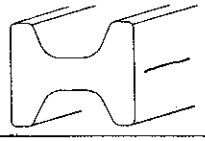	Minimizing the gap at the seam of mold copper Uniform cooling in the seam portion Powder casting
Internal cracks in web 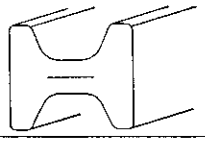	Intensive spray cooling in web portion Strict maintenance of roll gap
Internal cracks in flange tip 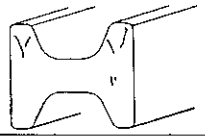	Intensive spray cooling in web portion Decreasing sulfur content in steel Strict maintenance of roll gap

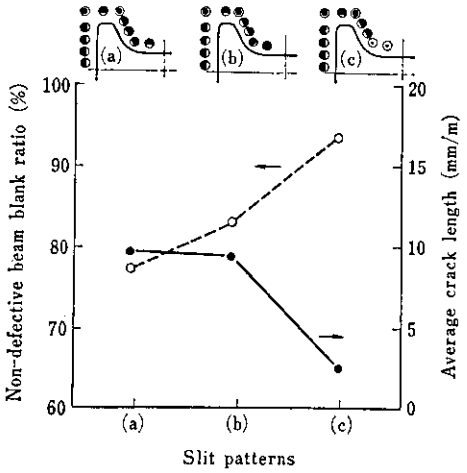

Fig. 7 Comparison of mold slit patterns in longitudinal cracks at web

Fig. 7 Comparison of mold slit patterns in longitudinal cracks at web

4 Defects Caused by High-speed Casting and Their Prevention

In the beam blank strand supporting method, the web and flange are supported only to 8 m below the meniscus and the shape of strand deteriorates as the casting speed increases, resulting in the cross section defects[4,6].

4.1 Defects in Cross Section

Photo. 1 shows a macrophotograph of cross section of the beam blank strand which has typical defects in the cross section. The main crack appears in the center of thickness in the web. Other smaller internal cracks are observed at the flange tip and web. **Fig. 8** shows the effects of casting speed and the sulfur contents in molten steel on internal cracks in the web. This figure indicates that cross-section cracks are more liable to occur as the sulfur content in molten steel increases

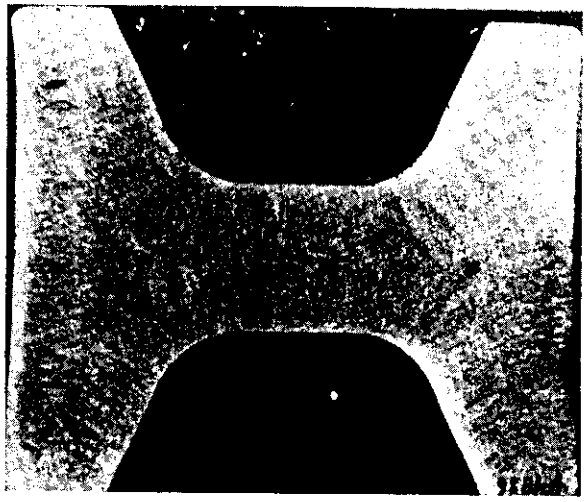

Photo. 1 Internal Crack in web

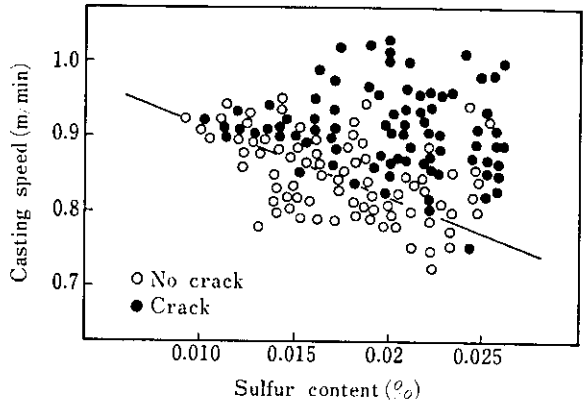

Fig. 8 Effects of casting speed and sulfur content on internal cracks in web

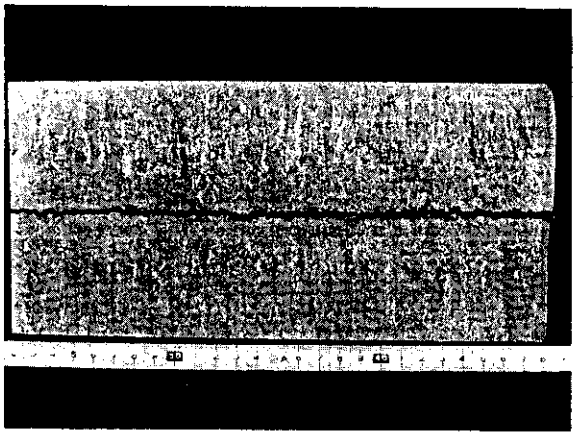

Photo. 2 Internal crack in web

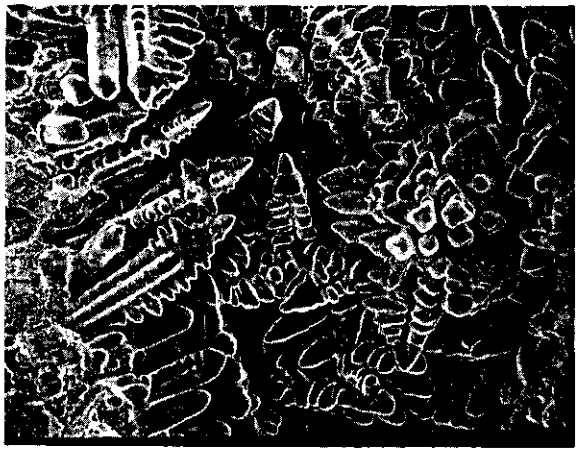

Photo. 3 Electron microphotograph of internal crack surface

Photo. 4 Sulfur print of a bulging defect caused by ferrostatic pressure at the fillet of a blank due to excessive casting speed

and as casting speed rises. **Photo. 2** shows cross section defects in the web. The shapes of fracture at the upper and lower shells are very similar, thereby indicating the possibility of fracture after web solidification. **Photo. 3** shows an electron microphotograph of the fracture of cross-section cracking. The photo shows dendritic solidified surfaces. Regarding similar defects on the cross section of the slab, it is known that they are shrinkage cavities near the crater end and there is a dangerous zone where center cracks are liable to occur[7]. The cross-section cracks in the beam blank are considered to be similar defects.

In the case of the beam blanks, critical casting speed varies depending upon the strand supporting methods; when casting speed becomes higher than the critical casting speed, there occurs abnormal bulging as shown in **Photo. 4**. The shape of beam blank is so complex that strand deformation develops during the solidification process and the cooling process after the completion of solidification, thereby cross section cracks are liable to develop in the web. Thus it is considered that solidified shrinkage cavities tear during the cooling process and develop into cross section cracks. In order to prevent abnormal bulging and cross section cracking, therefore, it is considered effective to prevent stand deformation by employing the most suitable strand supporting method. In examining the optimum strand supporting method, the following analyses have been made regarding solidification of the beam blank strand and stress distribution inside the shell.

4.2 Solidification of Beam Blank Strand

In order to analyze the solidification of the beam blank strand, the 2-dimensional heat transfer analysis on a quarter cross section perpendicular to the casting direction as shown in **Fig. 9**, has been made by the direct difference method[8]. In this model, the flow of molten steel is ignored. The boundary conditions are shown in **Fig. 10**. In this figure, the cooling zones are divided into 3 areas, i.e., the spray cooling zone, the splashing and flowing water cooling zone and natural cooling zone, and heat transfer has been made into patterns in respect of the 3 zones for calculation purposes. Changes in solidified shell thickness are shown in **Fig. 11**. In this figure, the measured values of the breakout shell are also given. The calculation results show good agreement with measured values, thereby confirming the validity of the model.

Fig. 12 shows the progress in solidification of the shell calculated by using this model.

From the results of this calculation, the following points have been clarified:

(1) Flange tip solidifies at an early stage.
(2) The final solidifying position lies at the fillet which

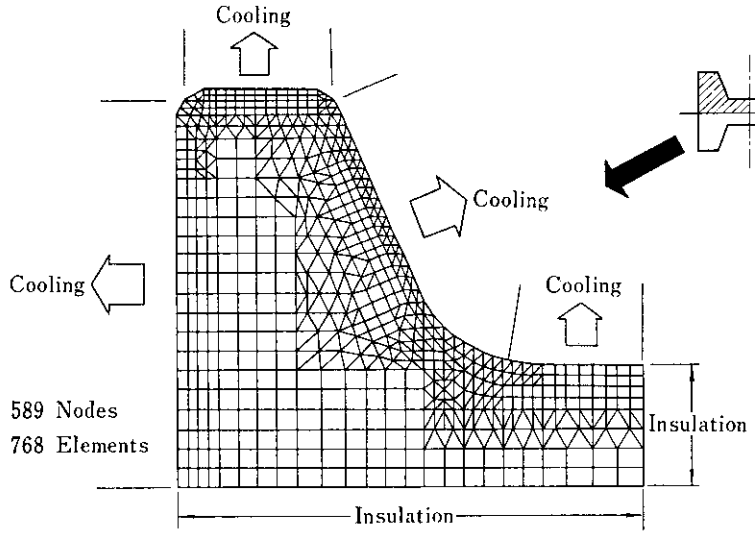

Fig. 9 Modelling for heat transfer analysis

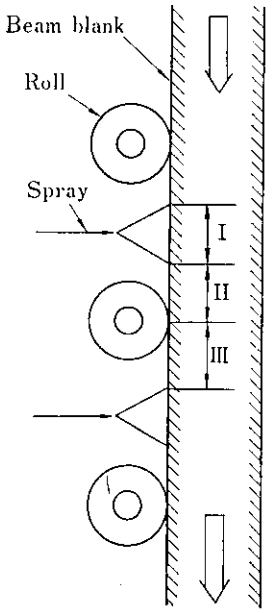

I. Spray cooling

Heat flux : $Q=h\cdot(\theta_S-\theta_a)$ (kcal/m²·h)

$h=2.83\cdot10^4\cdot W^{0.75}/\theta_S^{1.2}+100$ (kcal/m²·h·°C)

θ_S, θ_a : Temperature (Surface, Atmosphere)

W: Flow rate per spray area (l/m²·min)

II. Cooling by splashing and flowing water

$Q=h\cdot(\theta_S-\theta_a)$

$h=513\cdot(k_1\cdot\gamma)^{1/3}$

$k_1=0.06$ (const.)

γ : Flow rate per unit width [l/m·min]

III. Natural cooling

$$Q=4.88\cdot\varepsilon\cdot\left[\left(\frac{\theta_S+273}{100}\right)^4-\left(\frac{\theta_a+273}{100}\right)^4\right]+2.2\cdot|\theta_S-\theta_a|^{1/4}(\theta_S-\theta_a)$$

ε : Emissivity [——]

Fig. 10 Heat transfer for beam blank strand

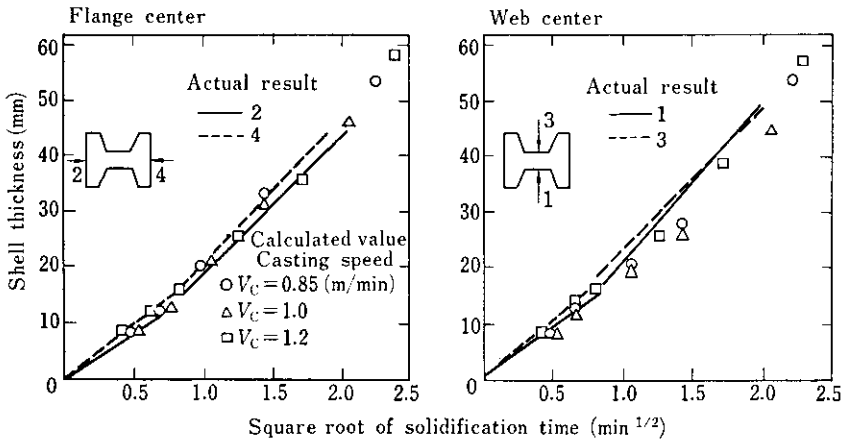

Fig. 11 Comparison of calculated and actual shell thickness

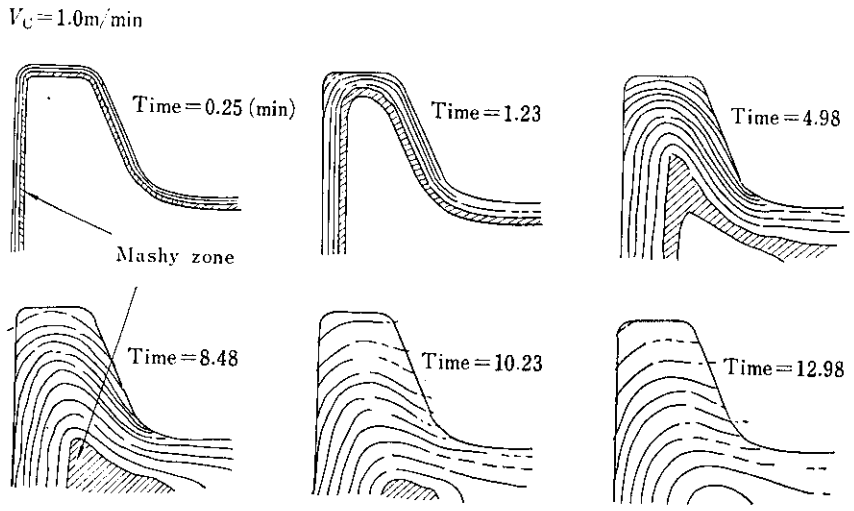

Fig. 12 Progress of solidification of C. C. beam blank by calculation

is about 100 mm away from the center of the flange surface.

(3) As the solidification of the web progresses, the shape of molten steel near the crater end changes from an acute-angled triangle to an ellipse.

(4) At the final stage of solidification, accelerated solidification is observed.

4.3 Stress Distribution in the Shell of Beam Blank

Since the beam blank has a complex shape, stress inside the shell during solidification and cooling is considered to be affected by the strand support method. In order to investigate stress distribution inside the solidified shell, 2- and 3-dimensional elastic stress analyses of the shell have been performed by the finite element method. Since stress in the solidified shell is in the plastic region, it would be necessary, strictly speaking, to make an elasto-plasticity analysis. However, when 2-dimensional elasticity and elasto-plasticity analyses of the shell are performed, no difference has been observed between them in the trend. Therefore, as far as relative measure is concerned, the elasticity analysis has been considered sufficient.

In the present analysis, stress in the solidified shell caused by the static pressure of molten steel has been mainly examined. For the localized point such as the flange tip, a 2-dimensional analysis has been performed, while the quantities of strain and displacement due to bulging arising from the static pressure of molten steel have been evaluated by means of the 3-dimensional analysis of the shell.

Main conditions used in the calculations are given below.

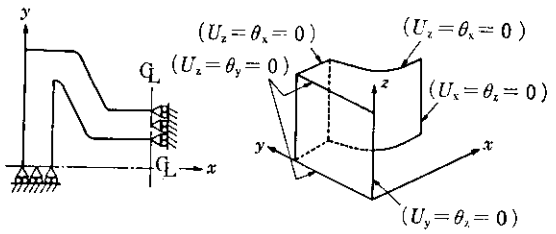

(a) 2-dimensional analysis (b) 3-dimensional analysis

U : Displacement, θ : Revolution angle

Fig. 13 Boundary condition of finite element model

(1) Strand supporting conditions
For the finite element model, a quarter cross section perpendicular to the casting direction has been taken out and given supporting conditions that will satisfy the symmetrical conditions. An example of the supporting conditions is given in **Fig. 13**.

(2) Strand temperature and solidified shell thickness
Temperature distribution in the shell is assumed as a straight line; and for the surface temperature, measured values in **Fig. 14** have been employed.

(3) Solidified shell thickness
Solidified shell thickness (mm) is obtained from the breakout shell thickness by using the following equations:

$$\text{Flange center:}\quad d_1 = 25.0\sqrt{t} - 5.5$$
$$\text{Web center :}\quad d_2 = 27.5\sqrt{t} - 4.8$$

(t: Casting time in min.)

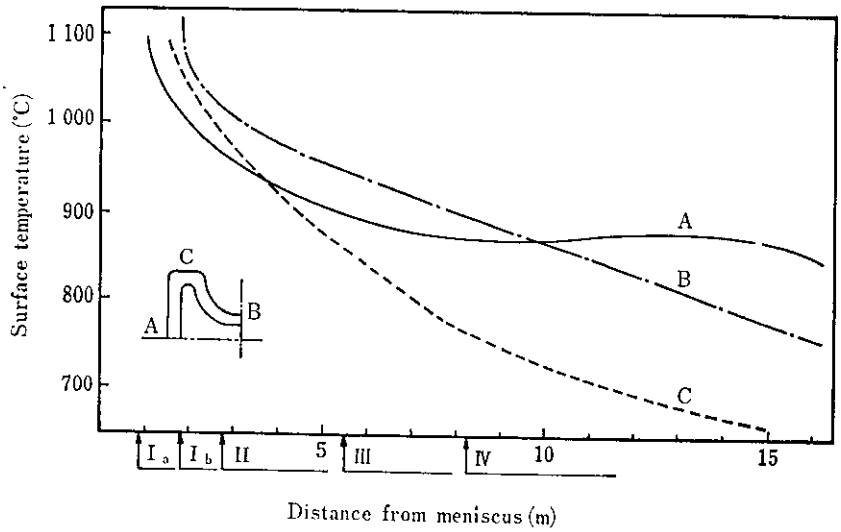

Fig. 14 Surface temperature of cast steel

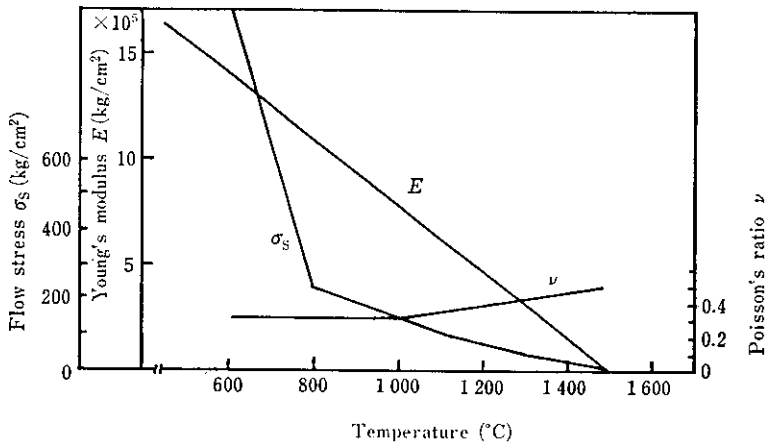

Fig. 15 Mechanical properties of cast steel

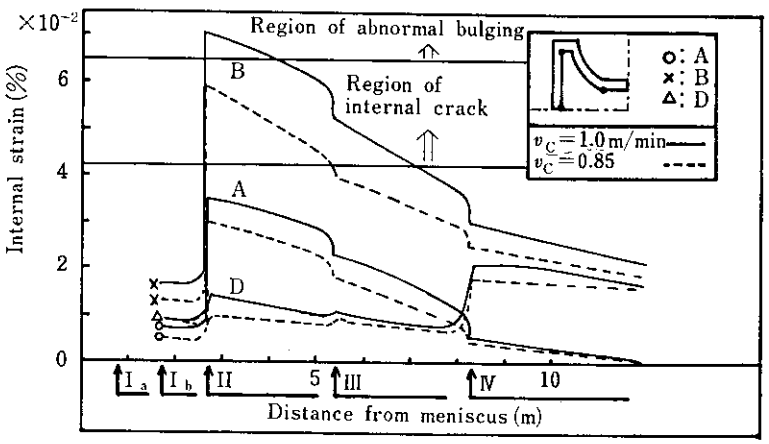

Fig. 16 Internal strain distribution in strand direction in the case of supporting way of cast blanks shown in Fig. 4

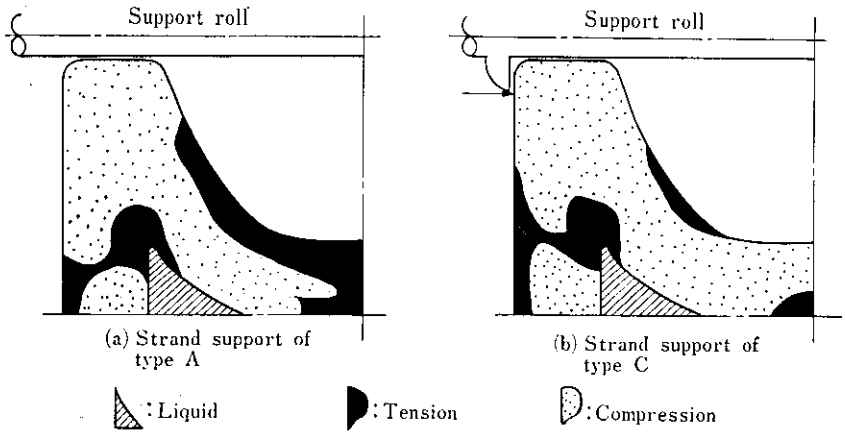

Fig. 17 Stress distribution of beam blank at No. 4 segment

(4) Physical property constants

The values of physical properties, Poisson's ratio, Young's modulus and deformation resistance shown in **Fig. 15** have been employed. These values are obtained from the data by K.A. Fekete[9] and other's.

The calculation results are given below.

Fig. 16 shows the transition of maximum values of internal strain on the solidified boundary in the casting direction. In this case, the strand supporting method is employed as shown in **Fig. 4**. The values of maximum strain become smaller in the order of the tip corner (Point B), flange center (Point A) and web (Point D), and decrease as solidification progresses. In previous experiences, internal cracks occurred at Point B, but not at Point A, with abnormal bulging shown in **Photo. 4** sometimes occurring when casting speed exceeded 0.9 m/min. After evaluating internal cracks by internal strain at each part the permissible values of respective internal strains have been estimated from operation results under various operating conditions. The results are also shown in **Fig. 16**.

Fig. 17 shows stress distribution at the section below 8 m from the meniscus. **(a)** shows the use of the present supporting method shown in **Fig. 4**, and **(b)** illustrates the tip supporting method from the flange face for the purpose of preventing warping of the flange. This suggests that the improvement of supporting methods has expanded the compressive stress regions of the fillet and web, and is effective in preventing bulging.

4.4 Cast Supporting Method and Casting Speed

From the results of the foregoing examinations, it has been clarified that selection of a suitable strand supporting method can prevent the occurrence of abnormal bulging, and casting speed can be increased without bulging.

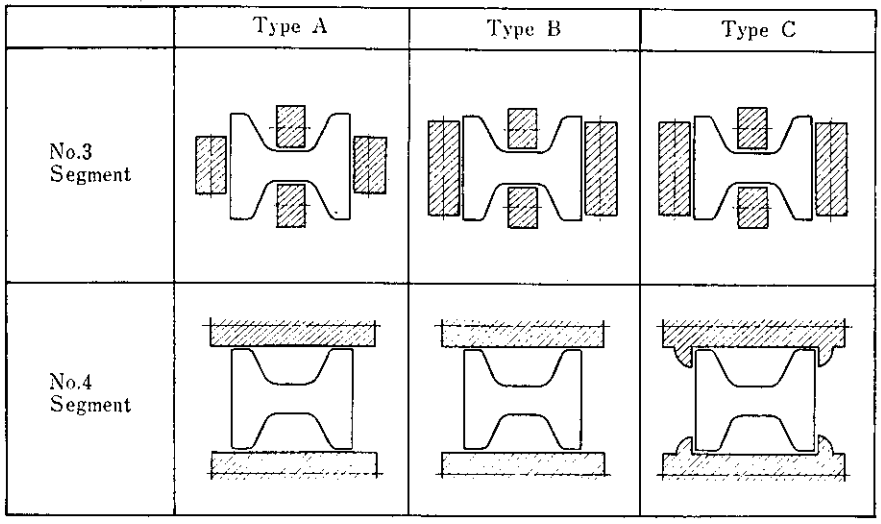

Fig. 18 Types of strand supports

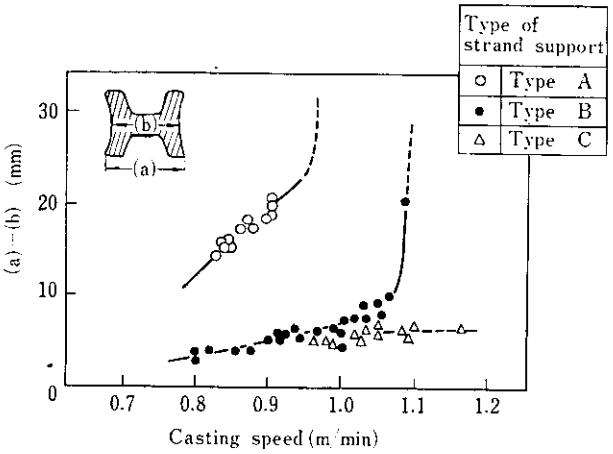

Fig. 19 Relation between casting speed and deformation of B. B.

Experiments of high-speed casting have been conducted by employing the strand supporting methods shown in **Fig. 18,** and the results are shown in **Fig. 19.** When the entire flange surface is supported to 8 m below the meniscus as in Type B, the quantity of strand deformation "(a)–(b)" becomes about 1/5 of that by the conventional method, with the casting speed made to be increased from 0.85 to 1.0 m/min without abnormal bulging. Next, when the side support is further extended by 2.7 m by using special roll as shown in Type C, it becomes possible to achieve a casting speed of 1.2 m/min without any deterioration to the quality and shape of the strand. As shown above, it has been clarified that difference in the strand supporting method will cause a difference in critical casting speed at which the strand is deformed with abnormal bulging. The above suggests that improvement of the supporting method can further increase the casting speed.

5 Operation of Beam Blank CC Machine

5.1 Operation Results

Table 4 shows the operational results of the beam blank continuous casting machine. The ratio of casting time has reached 90.4% and product yield for 40 kg/mm² steel is as high as 99.6%. This is due to the stabilized operation, as can be clearly seen from the low frequency of breakouts and the high ratio of ladle empty. Further, the number of heats in sequence per tundish as high as 10.9 and the number of heats in sequence per dummy bar as high as 36.4 have contributed to the above achievement in the ratio of casting time and yield. As mentioned above, the tundish has no device for flow rate control, and casting speed is controlled by the bore of tundish nozzles and

Table 4 Operational results

Item	Results
Ratio of casting time (%)	90.4
Yield (%)	99.6*
Frequency of breakouts (%)	0.02
Ratio of completed heats (%)	100
Number of heats in sequence per tundish	10.9
Number of heats in sequence per dummy bar	36.4

('79 July-Dec.) *40 kg/mm² grade

Table 5 Typical properties of tundish nozzle

Properties \ Classification		Present type	Conventional type
Apparent porosity (%)		14.6	12.6
Water absorption (%)		3.0	3.2
Apparent density		5.63	4.52
Bulk density		4.81	3.94
Crushing strength (kgf/cm²)		1 150	1 373
Refractoriness under load T_2 (°C)		>1 700	>1 700
Thermal expansion (%)		0.64 at 1 500°C	0.35 at 1 000°C 0.75 at 1 500°C
Permanent linear change at 1 500°C×2 h (%)		0	0
Chemical composition (%)	SiO_2	0.6	33.6
	Al_2O_2	0.5	1.1
	Fe_2O_3	0.5	0.2
	ZrO_2	94.0	64.5
	CaO	4.0	

the depth of molten steel in the tundish. Therefore, a decrease in the number of sequence casting per tundish is caused by nozzle bore changes. It is, therefore, important to make proper selections of the material and shape of nozzles. In the present beam blank casting, the adoption of zirconia nozzles has remarkably improved the number of heats in sequence per tundish, attaining 16 to 17 continuous continuous castings. **Table 5** shows a comparison in typical properties between the present and conventional types of tundish nozzels.

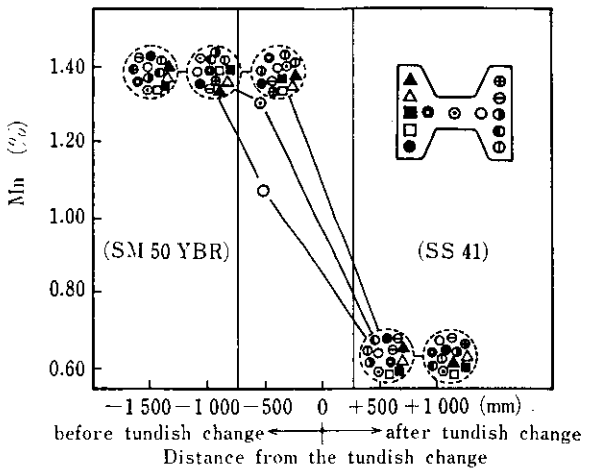

Fig. 20 Change of chemical composition at tundish change

For continuous continuous casting of different types of steel, tundish change is performed without any device to separate molten steel of different compositions. **Fig. 20** shows changes in chemical composition by this method, and the mixing region is about 1 m in length. The continuous continuous casting of the same type and different types of steel by tundish change has greatly increased the number of heats in sequence per dummy bar, thereby achieving 142, the highest number of heats in sequence.

5.2 Continuous Casting Condition of Materials for H-shapes

The present stage of continuous casting of materials for H-shapes at Mizushima Works is described below. In Mizushima Works, the "rolling techniques for manufacturing multisized H-shapes from single-sized beam blanks"[10] and "rolling techniques for manufacturing large-sized H-shapes from slabs"[11] have been successfully developed. The continuous casting ratio of materials for H-shapes reached 98.2% in December, 1979. **Fig. 21** shows the product sizes classified by production process of H-shapes. The development of rolling techniques of these materials for H-shapes has greatly expanded the range of types of steel suitable for continuous casting, thereby greatly contributing to a reduction in the product cost.

Continuously cast beam blanks occupy 64% of materials for H-shapes, with CC blooms and CC slabs accounting for the remainder.

Along with expansion in rolling sizes from single-sized beam blanks, rolling conditions of raw materials have become stricter and quality requirements for beam blanks have become severer. Nevertheless, the no-conditioning rate has exceeded 99% and the hot charging rate has reached 80%, maintaining a very satisfactory quality level.

6 Conclusions

Examinations have been made on strand deformation and the optimum strand supporting method, with the aim of increasing casting speed in order to increase the capacity of the beam blank CC machine. The results obtained by the examinations are given below.

(1) Values of surface temperature transition, shell thickness variation, etc., which have been obtained from the model calculations have shown good agreement with measured values.

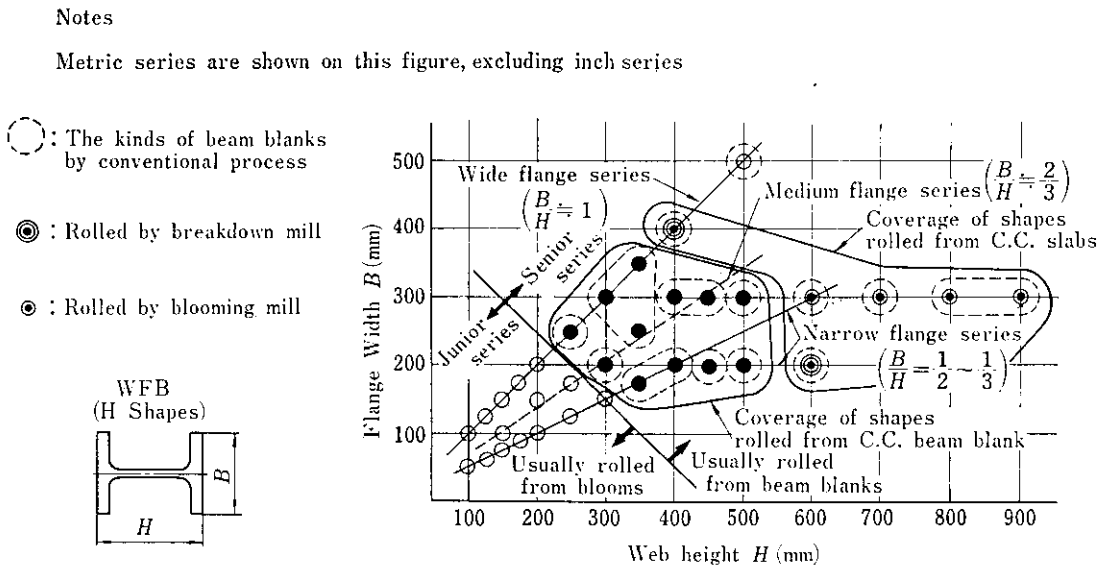

Fig. 21 Relation between wide flange beam sizes and materials

(2) As web solidification progresses, the shape of molten steel near the crater end changes from an acute-angled triangle to an ellipse.

(3) The internal stress of beam blanks calculated by the elasticity analysis can be improved by employing the cast supporting method which prevents the flange deformation.

(4) As a result of employing the cast supporting method which prevents flange warping, it has become possible to increase the casting speed from 0.85 to 1.2 m/min without deteriorating quality of cast blanks.

Regarding surface and internal quality, it is also important to control operating conditions such as cooling conditions, mold powder selection, and enhancing of machine maintenance.

At present, the no-conditioning ratio of raw materials is maintained at a level of over 99%. Further, frequency of breakouts is lower and the complete casting ratio (the ratio of the number of emptied ladles to total number of ladles cast) is 100%.

With the improvement in the number of heats in sequence, the ratio of availability has reached 90.4%, thereby achieving a stabilized operating record.

At the Mizushima Works, the "rolling techniques for manufacturing multi-sized H-shapes from single-sized beam blanks" and "rolling techniques for manufacturing largesized H-shapes from slabs" have been successfully developed, thereby greatly expanding the range of steel types suitable for continuous casting and raising the ratio of continuous-cast materials for H-shapes to almost 100%.

References

1) M. Kodama, T. Chino and H. Koide: *Kawasaki Steel Technical Report*, **7** (1975) 2, pp. 15–23 (in Japanese)
2) T. Nozaki, K. Murata, H. Ooi and M. Kodama: *Tetsu-to-Hagané*, **60** (1974) 11, S462
3) T. Nozaki, T. Itami, K. Murata, J. Matsuno, M. Fukai and M. Kodama: *Kawasaki Steel Technical Report*, **9**(1977) 3·4, pp. 11–21 (in Japanese)
4) Y. Iida, H. Moriwaki, T. Ueda, T. Fujimura, M. Ariyoshi and H. Mizota: *Tetsu-to-Hagané*, **65** (1979) 11, S759
5) K. Emoto, M. Kodama, M. Fukai, T. Nozaki and T. Yoshikado: *Kawasaki Steel Technical Report*, **9** (1977) 3·4, pp. 22–32 (in Japanese)
6) T. Saito, M. Kodama and K. Komoda: *Iron Steel Intern.*, **48** (1977) 5, p. 391
7) S. Harada, A. Kusano and H. Misumi: *Seitetsu Kenkyu*, **294** (1978), p. 72
8) M. Yao: The 24th Chugoku and Shikoku Conference of *Iron and Steel Institute*, **3** (1974), p. 135
9) K.A. Fekete: *Radex Rundschau* (1974) 3, p. 135
10) T. Tanaka, M. Yamashita, T. Agune, H. Nagahiro, K. Hitomi and T. Kusada: *Kawasaki Steel Technical Report*, **10** (1974) 4, pp. 69–78 (in Japanese)
11) T. Tanaka, M. Yamashita, S. Sato, E. Yamanaka, H. Nagahiro and N. Kuriyama: *Tetsu-to-Hagané*, **56** (1980) 4, S273